

3DRealCar: An In-the-wild RGB-D Car Dataset with 360-degree Views

Xiaobiao Du^{1,2,3} Yida Wang³ Haiyang Sun³ Zhuojie Wu¹ Hongwei Sheng¹
Shuyun Wang¹ Jiaying Ying¹ Ming Lu⁵ Tianqing Zhu⁴ Kun Zhan³ Xin Yu^{1*}

¹ The University of Queensland ² University of Technology Sydney ³ Li Auto Inc.
⁴ City University of Macau ⁵ Peking University

Abstract

3D cars are commonly used in self-driving systems, virtual/augmented reality, and games. However, existing 3D car datasets are either synthetic or low-quality, limiting their applications in practical scenarios and presenting a significant gap toward high-quality real-world 3D car datasets. In this paper, we propose the first large-scale 3D real car dataset, termed 3DRealCar, offering three distinctive features. (1) **High-Volume**: 2,500 cars are meticulously scanned by smartphones, obtaining car images and point clouds with real-world dimensions; (2) **High-Quality**: Each car is captured in an average of 200 dense, high-resolution 360-degree RGB-D views, enabling high-fidelity 3D reconstruction; (3) **High-Diversity**: The dataset contains various cars from over 100 brands, collected under three distinct lighting conditions, including reflective, standard, and dark. Additionally, we offer detailed car parsing maps for each instance to promote research in car parsing tasks. Moreover, we remove background point clouds and standardize the car orientation to a unified axis for the reconstruction only on cars and controllable rendering without background. We benchmark 3D reconstruction results with state-of-the-art methods across different lighting conditions in 3DRealCar. Extensive experiments demonstrate that the standard lighting condition part of 3DRealCar can be used to produce a large number of high-quality 3D cars, improving various 2D and 3D tasks related to cars. Notably, our dataset brings insight into the fact that recent 3D reconstruction methods face challenges in reconstructing high-quality 3D cars under reflective and dark lighting conditions. [Our dataset is here.](#)

1. Introduction

Cars, as both daily objects and vehicles, are of significant interest to researchers, especially in the field of autonomous driving. Autonomous perception systems are typ-

ically trained on daily scene datasets that are collected frequently. However, these datasets often exhibit long-tailed distributions, with far fewer instances of corner-case scenarios, like car accidents. Consequently, this imbalance leads to the autonomous perception system generalizing well in the most frequently occurring scenes. This means that the system is likely to perform poorly in rare situations, posing significant safety risks to drivers. To build a reliable system, it is essential to have a simulator that can simulate photorealistic hazardous scenes. Moreover, high-quality 3D cars are necessary for a realistic simulator.

Recent 3D car reconstruction methods mainly reconstruct cars from self-driving datasets. To apply reconstructed cars to real-world scenes, the reconstructed 3D car should be high-quality. However, it is very challenging to obtain such high-quality 3D cars for the following reasons: (1) Previous 3D car reconstruction methods produce low-quality 3D cars, primarily because they train on self-driving datasets with low-resolution car images and a limited number of trainable views. (2) Manually crafting a high-quality 3D car model requires specialized artists, which is time-consuming. (3) There is no large-scale 3D real car dataset that can be utilized to produce a bulk of 3D cars.

Moreover, existing 3D car datasets are either synthetic or only contain a few posed images, as shown in Figure 2. SRN-Car [6] and Objaverse-Car [8] collect 3D car computer-aided design (CAD) models from the Internet, but these models are synthetic and contain non-photorealistic texture. Although MVMC [50] is a real car dataset, it collects only ten views on average for each car. On the contrary, our collected 3DRealCar dataset provides an average of 200 dense RGB-D views per car for high-quality 3D car reconstruction.

We also show that the recent state-of-the-art 3D generative method, MVDream [38], as depicted in Figure 2, fails to generate high-quality cars due to the multi-view inconsistency introduced by generative models. Thus, the existing 3D generation methods cannot be employed to generate high-quality 3D real car assets.

In this work, we collect a large-scale 3D real car dataset

*Corresponding author.

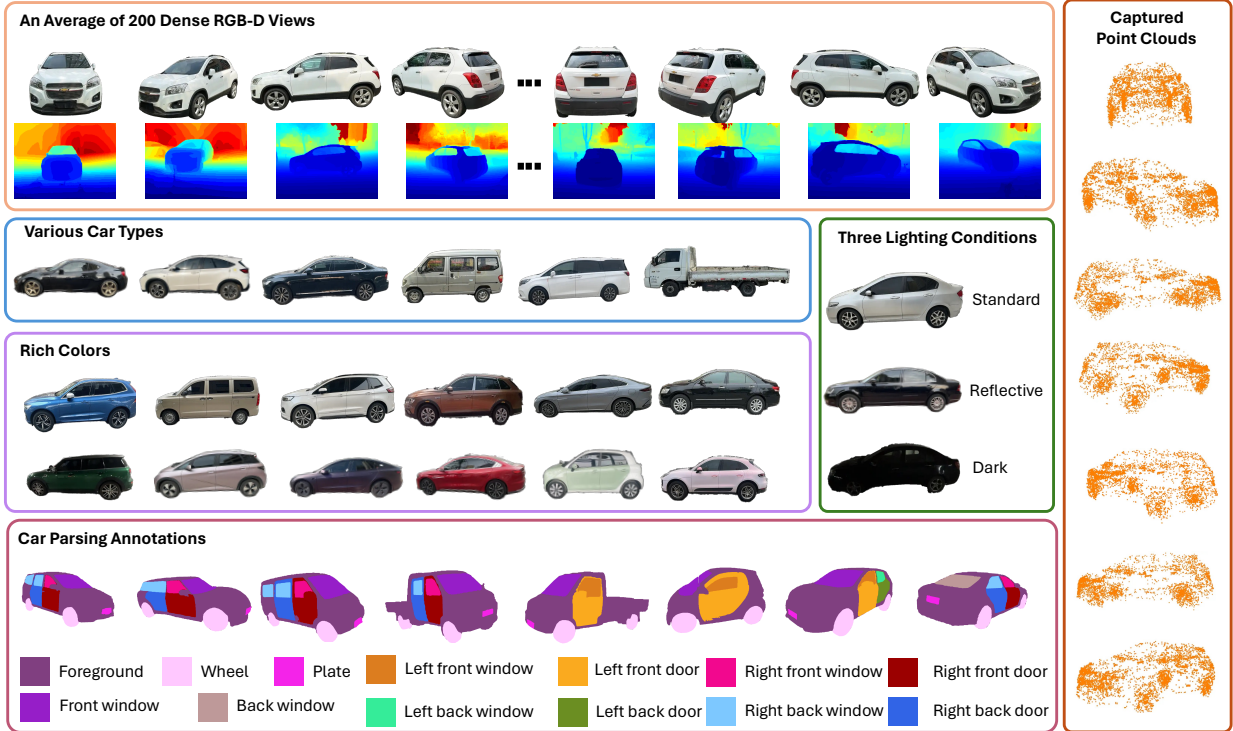


Figure 1. **Characteristics of our curated high-quality 3DRealCar dataset.** 3DRealCar contains detailed annotations for various colors, car types, brands, and car parsing maps. 3DRealCar contains three lighting conditions on car surfaces, bringing challenges to existing methods. Table 1. **The comparison of existing 3D car datasets.** Our dataset contains unique characteristics compared with existing 3D car datasets. Lighting means the lighting conditions of the surfaces of cars. Point Cloud represents the point clouds with actual sizes in real-world scenes.

Dataset	Instances	Type	Views	Resolution	Brand	Lighting	Car Parsing	Depth	Point Cloud
SRN-Car	2151	Synthetic	250	128×128	×	×	×	×	×
Objaverse-car	511	Synthetic	-	-	×	×	×	×	×
MVMC	576	Real	~10	600×450	~40	×	×	×	×
3DRealCar (Ours)	2500	Real	~200	1920×1440	100+	3	13	✓	✓

in the wild, termed 3DRealCar, which contains dense high-quality views and rich diversity. During data collection, we employ smartphones with ARKit [2] to scan cars parked on roadsides or parking lots, obtaining posed RGB-D images and point clouds of cars. In particular, we scan around the cars in three loops to obtain dense views. Note that we collect car data with the consent of owners. In Table 1 and Figure 1, we show our dataset possesses striking characteristics compared with previous 3D car datasets. We capture dense RGB-D images in high resolution, which promotes the reconstruction of high-quality 3D cars. Furthermore, we scan cars under three different lighting conditions, resulting in the surfaces of cars having different lighting effects, such as reflective, standard, and dark, where we denote the standard as the smooth lighting condition without obvious specular highlight. Figure 2 shows some examples of three lighting conditions in our dataset. Note that the number of instances in our dataset is the largest in existing datasets.

Therefore, our collected 3DRealCar dataset has a rich diversity in terms of car types, colors, brands, and lighting conditions. We also provide car parsing map annotations with thirteen classes for each instance, which enable our dataset to be applied in car component understanding tasks.

To construct a high-quality dataset, we filter out the images that are out of focus, occluded, or blurred. To facilitate the 3D reconstruction solely on cars, we remove the point clouds of the background. We also adjust the orientation of the car facing along the x-axis before the reconstruction for controllable rendering. Based on the high-quality posed RGB-D images, point clouds, and multi-grained annotations, we can apply the dataset to various tasks related to cars. Figure 3 shows our dataset supports over 10 tasks, including several popular 2D and 3D tasks to promote the advancement of car-related research.

We leverage existing state-of-the-art methods to benchmark 3D reconstruction and car parsing tasks of our 3DReal-



Figure 2. **Visual comparisons of 3D car datasets and the results of a 3D generative method.** Our 3DRealCar is captured in real-world scenes and contains more densely captured views. In addition, our dataset has annotations for three different lighting conditions on the car surface. We also compare a recent state-of-the-art text-to-3D model, MVDream [38] with a prompt “a modern sedan”, demonstrating its failure to generate high-quality 3D car models.

Car dataset. We also conduct extensive experiments to demonstrate that the reflective and dark lighting conditions in our dataset are challenging to existing methods, which brings a new challenge for 3D reconstruction in awful lighting conditions. Furthermore, we demonstrate that our 3DealCar dataset can bring real-car prior and enhance existing 3D generation and downstream methods. Overall, the contributions of this work can be summarized below:

- We propose the first large-scale 3D real car dataset, named 3DRealCar, which contains 2,500 car instances and their point clouds with actual sizes in real-world scenes.
- 3DRealCar contains RGB-D images and point clouds with detailed annotations, supporting researchers to investigate various tasks in both 2D and 3D.
- We conduct 3D reconstruction and car parsing benchmarks to advance car-related tasks. Notably, we observe that existing methods face challenges under the extreme lighting conditions of 3DRealCar.
- Extensive experiments demonstrate 3DRealCar can enhance real-car prior and improve the performance of existing 3D generation and novel view synthesis methods.

2. Related Work

3D Car Datasets. There are several well-known large-scale autonomous driving datasets so far, such as Nuscenes, KITTI, Waymo, Pandaset [48], ApolloScape [14], and Cityscape. These datasets are captured by multi-view cameras and lidars mounted on ego cars. Various works [10, 12, 45] attempt to reconstruct 3D cars in these datasets. However, these methods fall short of reconstructing high-quality 3D cars due to the lack of sufficient and dense training views. SRN-Car [6] and Objaverse [8] collect 3D car models from existing repositories and Internet sources. However, these datasets only contain synthetic cars, which cannot produce

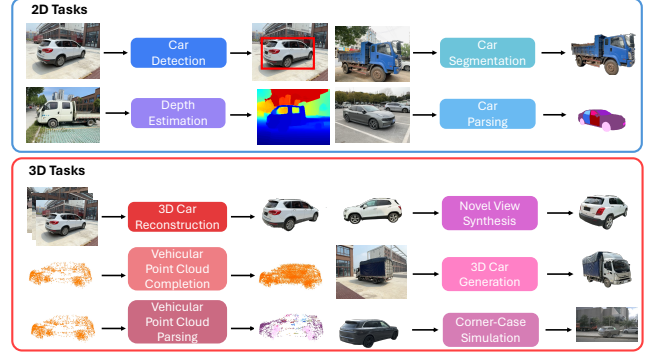


Figure 3. **The applicable tasks of our dataset.** Our proposed 3DRealCar dataset containing RGB-D images, point clouds, and rich annotations, can be applied to various popular 2D and 3D tasks to support the construction of safe and reliable self-driving systems.

realistic textures and geometry. MVMC [50] is collected from car advertising websites, which contain a series of car images, especially multi-view images of each car. However, the views of images per car in MVMC are unposed and sparse, which is adverse to reconstructing high-quality 3D car models. In this paper, we collect a high-quality 3D real car dataset to fill the above gaps.

3D Reconstruction with Neural Field. 3D reconstruction aims to create a 3D structure digital representation of an object or a scene from its multi-view images, which is a long-standing task in computer vision. One of the most representative works in 3D reconstruction is Neural Radiance Fields (NeRFs) [28], which demonstrates promising performance for novel view synthesis. Afterward, this method inspires a new wave of 3D reconstruction methods using the volume rendering method, with subsequent works focusing on improving its quality [46], efficiency [7], applying artistic effects, and generalizing to unseen scenes. Particularly, Kilonerf [35] accelerates the training process of NeRF by dividing a large MLP into thousands of tiny MLPs. Furthermore, Mip-NeRF [3] proposes a conical frustum rather than a single ray to ameliorate aliasing. Mip-NeRF 360 [4] further improves the application scenes of NeRF to the unbounded scenes. Although these NeRF-based methods demonstrate powerful performance on various datasets, the training time always requires several hours even one day more. Instant-NGP [30] uses a multi-resolution hash encoding method, which reduces the training time by a large margin. 3DGS [17] proposes a new representation based on 3D Gaussian Splatting, which reaches real-time rendering for objects or unbounded scenes. 2DGS [13] proposes a perspective-accurate 2D splatting process that leverages ray-splat intersection and rasterization to further enhance the quality of the reconstructions. Scaffold-GS [26] proposes an anchor growing and pruning strategy to accelerate the scene coverage. MVGS [11] firstly proposes the multi-view training strategy to optimize 3DGS in a more comprehensive

way for holistic supervision. However, there is not yet a large-scale 3D real car dataset so far. Therefore, we present a 3D real car dataset, named 3DRealCar in this work.

3D Generation with Diffusion Prior. Some current works [16, 31] leverage a 3D diffusion model to learn the representation of 3D structure. However, these methods lack generalization ability due to the scarcity of 3D data. To facilitate 3D generation without direct supervision of 3D data, image or multi-view diffusion models are often used to guide the 3D creation process. Notable approaches like DreamFusion [34] and subsequent works [27] use an existing image diffusion model as a scoring function, applying Score Distillation Sampling SDS loss to generate 3D objects from textual descriptions. These methods, however, suffer from issues such as the Janus problem [34] and overly saturated textures. Inspired by Zero123 [22], several recent works [37, 39] refine image or video diffusion models to better guide the 3D generation by producing more reliable multi-view images. However, these generative methods fail to generate high-quality cars without the prior of real cars.

3. Proposed 3DRealCar Dataset

3.1. Data Collection and Annotation

As shown in Figure 4, our dataset is collected using smartphones, specifically iPhone 14 models, adopting ARKit APIs [2] to scan cars for their point clouds and RGB-D images. The data collection process is conducted under three distinct lighting conditions, such as standard, reflective, and dark. These lighting conditions represent the lighting states of vehicle surfaces. It is important to note that all data collection is performed with the consent of owners. During the scanning process, the car should be stationary while we meticulously circle the car three times to capture as many views as possible. For each loop, we adjust the height of the smartphone to obtain images from different angles. Furthermore, we try our best to make sure captured images contain the entire car body without truncation. To preserve the privacy of owners, we make license plates and other private information obfuscated. To construct a high-quality dataset, we filter out some instances with blurred, out-of-focus, and occluded images. We also provide detailed annotations for car brands, types, and colors. Particularly, we provide the car parsing maps for each car with thirteen classes in our dataset as shown in Figure 1 for the advancement of car component understanding tasks.

3.2. Data Preprocessing

Background Removal. Since we only reconstruct cars for the 3D car reconstruction task, the background should be removed. Recent Segment Anything Model (SAM) [20] demonstrates powerful context recognition and segmentation performance. However, SAM needs a bounding box,

text, or point as a driving factor for accurate segmentation. Therefore, we employ Grounding DINO [23] as a text-driven detector with a detection prompt with “car” for the attainment of car bounding boxes. With these bounding boxes, we use SAM to obtain the masks from captured images. The point cloud initialization is demonstrated useful for the convergence of 3D Gaussian Splatting [18]. Except for the removal of the background in 2D images, we still need to remove the background point clouds. Therefore, we first project the 3D point clouds into 2D space with camera parameters. Then, we can eliminate background point clouds with masks and save them for further processing.

Orientation Rectification. As shown in Figure 4, we utilize Colmap [36] to reconstruct more dense point clouds and obtain accurate camera poses and intrinsics because we find that the estimated poses by the smartphone are not accurate. However, after the removal of the background point clouds, we find that the car orientation of the point cloud is random, which leads to the subsequent render task being uncontrollable. Given camera poses $P = \{p_i\}_1^N$, where N is the number of poses, we use Principal Component Analysis (PCA) [1] to obtain a PCA component $\mathcal{T} \in \mathbb{R}^{3 \times 3}$. The PCA component is the principal axis of the data in 3D space, which represents rotation angles to each axis. Therefore, we leverage it to rectify the postures of cars parallel to the x-axis. However, this process cannot guarantee cars facing along the x-axis. Therefore, in some failure cases, we manually interfere and adjust the orientation along the x-axis. With the fixed car orientation, we can control rendered poses for the subsequent tasks.

Point Cloud Rescaling. The size of the point clouds reconstructed by Colmap [36] does not match the real-world size, which inhibits the reconstruction of a practically sized 3D car. To address this, we calculate the bounding box of the scanned foreground point clouds to obtain its actual size in the real-world scene. Then, we rescale the rectified point clouds into the real size. In addition to the rescaling of the point clouds, we also need to adjust the camera poses. We rescale translations of camera poses using a scale factor calculated by the ratio of scanned point cloud size and Colmap point cloud size. After these rescaling processes, we use rescaled point clouds to reconstruct a 3D car model through recent state-of-the-art methods, like 3DGS [18].

3.3. Data Statistics

In our 3DRealCar, we provide detailed annotations for researchers to leverage our dataset for different tasks. During the data annotating, we discard the data with the number of views less than fifty. As we can observe in Figure 1 and 2, we collect our dataset under real-world scenes and meticulously scan dense views. Therefore, cars in our dataset possess dense views and realistic texture, which is necessary for the application in a real-world setting.

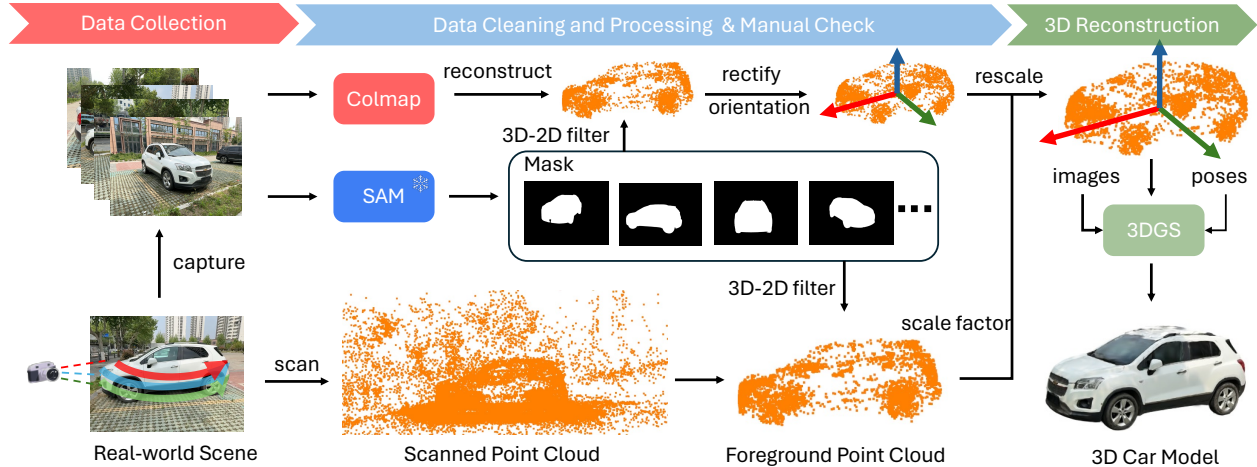


Figure 4. **Illustration of our data collection and preprocessing.** We first circle a car three times while scanning the car with a smartphone for the attainment of RGB-D images and its point clouds. Then we use Colmap [36] and SAM [20] to obtain poses and remove the background point clouds. Finally, we use the 3DGS [18] trained on the processed data to obtain 3D car model.

As shown in Figure 5, we conduct detailed statistical analyses to show the features of our dataset. Our dataset mainly contains six different car types, such as Sedan, SUV, MPV, Van, Lorry, and Sports Car. Among them, sedans and SUVs are common in real life, so their volume dominates in our dataset. We also count the number of different lighting conditions on cars. The standard condition means the car is well-lit and without strong highlights. The reflective condition means the car has strong specular highlights. Glossy materials bring huge challenges to recent 3D reconstruction methods. The dark condition means the car is captured in an underground parking so not well-lit. To promote high-quality reconstruction, we save the captured images in high resolution (1920×1440) and also capture as many views as possible. The number of captured images per car is an average of 200. The number of views ranges from 50 to 400. To enrich the diversity of our dataset, we try our best to collect as many different colors as possible. Therefore, our dataset contains more than twenty colors, but the white and black colors still take up most of our dataset. In addition, we also show the distribution of car size, in terms of their length, width, and height. We obtain their sizes by computing the bounding boxes of the scanned point clouds. Thanks to different car types, the sizes of cars are also diverse.

4. Overview of 3DRealCar Tasks

4.1. 2D tasks

Corner-case scene 2D Detection [44]: Given images $I = \{I_i\}_1^N$, this task aims to detect vehicles as accurately as possible. However, in some corner cases, like car accidents, detectors sometimes fail to detect target vehicles since this kind of scene is rare or not in the training set. Therefore, this task has crucial significance in building a reliable self-

driving system, especially for accident scenarios.

2D Car Parsing [25, 32, 47, 49]: Given a serial of images $I = \{I_i\}_1^N$, this task aims to segment car parsing maps $S = \{S_i\}_1^N$. With annotated parsing maps and images, we can train a model to understand and segment each component of cars. This task can assist self-driving systems with more precise recognition.

4.2. 3D Tasks

Neural Field-based Novel View Synthesis [13, 18, 29]: Given a serial of images $I = \{I_i\}_1^N$ and matched poses $P = \{p_i\}_1^N$, where N is the number of images and poses, the task of Neural Field-based Novel View Synthesis aims to reconstruct Neural Field model of a object or a scene. The reconstructed model is usually used to render 2D images with different views for the evaluation of the performance of novel view synthesis.

Diffusion-based Novel View Synthesis [22, 24, 39]: Given a serial of reference images $I^{ref} = \{I_i^{ref}\}_1^N$, reference poses $P^{ref} = \{p_i^{ref}\}_1^N$, target images $I^{target} = \{I_i^{target}\}_1^N$, and target poses $P^{target} = \{p_i^{target}\}_1^N$, recent 3D generative models, such as Zero123 [22], Syncdreamer [24], and Stable-Zero123 [39], take relative poses and reference images as inputs and generate target images. However, these models cannot generalize well to real car objects since they are trained on large-scale synthetic datasets [8, 9]. In this work, we will demonstrate that our dataset can improve the robustness of these generative models to real cars.

Single Image to 3D Generation [33, 42]: Given a text prompt or single image, recent 3D generation methods generate 3D objects with Score Distillation Sampling (SDS) [33] and diffusion generative models [22, 39]. However, these methods cannot generate high-quality 3D cars due to the

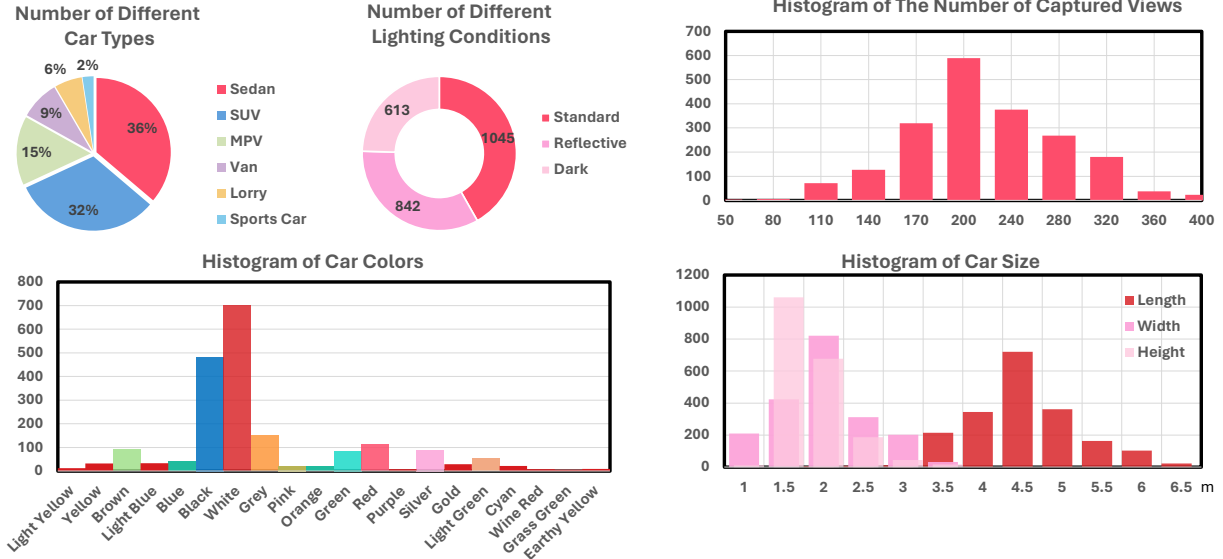


Figure 5. **The distributions of our 3DRealCar dataset.** We show distributions of car types, lighting conditions, captured views, car colors, and car size. We try our best to capture cars with various colors and types for the diversity of our dataset.

lack of the prior of real cars in 3D-based diffusion models. Therefore, we would demonstrate the value of our dataset by improving recent 3D generation for real cars.

5. Experiments

5.1. Experimental Setup

Corner-case 2D Detection. In this task, we leverage the reconstructed cars to simulate rare and corner-case scenes. To be specific, we use Nuscenes [5] as background to simulate corner-case scenes with reconstructed cars and leverage recent popular detectors, like YOLOv8 [44], as detectors for evaluation. To evaluate the robustness of detectors in corner-case scenes, we use the test part of the corner-case dataset, CODA [21] as a testing set. Since we focus on the corner-case scenes of cars, so we only evaluate a car class.

2D Car Parsing. In this task, we utilize DDRNet [32], SegFormer [49], VMamba [25], and InternImage [47] to benchmark our dataset. To be specific, we split 80% of our car parsing maps in 3DRealCar as the training set and the rest of 20% as the testing set.

Neural Field-based Novel View Synthesis. In this task, we randomly choose 100 instances from each lighting condition in our dataset and split 80% of the views per instance as the training set and the rest of 20% as the testing set. Specifically, we employ recent state-of-the-art neural field methods, including Instant-NGP [29], 3DGS [18], GaussianShader [15], and 2DGS [13] to benchmark our dataset.

Diffusion-based Novel View Synthesis. We finetune Zero123-XL [22] on our 3DRealCar dataset to enhance its generalization to real cars. Note that since the training of diffusion-based models needs entire objects centered on im-

ages, we use the images rendered by our trained 3D models as training images.

Single Image to 3D Generation. In this task, we exploit Dreamcraft3D [40] as our baseline. Dreamcraft3D exploits Stable-Zero123 [39] as a prior source for providing 3D generative prior. By fine-tuning Stable-Zero123 on our dataset, we enable it to obtain car-specific prior so it generalizes well to real cars.

5.2. Evaluation Metrics

PSNR \uparrow : Peak Signal-to-Noise Ratio (PSNR) is a metric of the peak error between the original and a compressed or reconstructed image. Higher PSNR values indicate better image quality, with a higher similarity to original images.

SSIM \uparrow : Structural Similarity Index (SSIM) is a perceptual metric that considers changes in structural information, luminance, and contrast between the original and target image. Higher SSIM values indicate better performance.

LPIPS \downarrow : Learned Perceptual Image Patch Similarity (LPIPS) is a metric that uses deep learning models to assess the perceptual similarity between images. Lower LPIPS values indicate higher perceptual similarity. Unlike PSNR and SSIM, LPIPS leverages the capabilities of neural networks to better align with human visual perception.

mAP \uparrow : In the object detection task, mAP denotes mean Average Precision, a widely used metric to evaluate the performance of detection algorithms. It measures the accuracy of the detector by considering both the precision and recall at different thresholds. Higher mAP means better results.

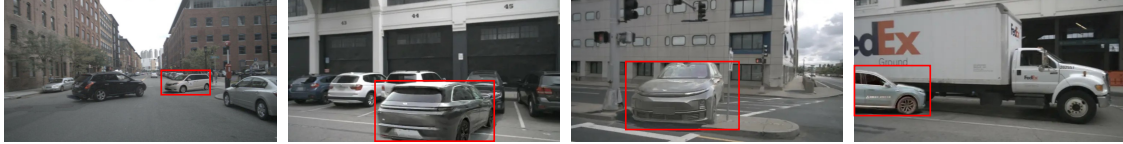


Figure 6. **The simulated corner-case scenes.** These scenes are rare but very important in real life. We use a red rectangle to highlight the simulated vehicles. These corner-case scenes show some vehicles have potential risks to traffic safety.

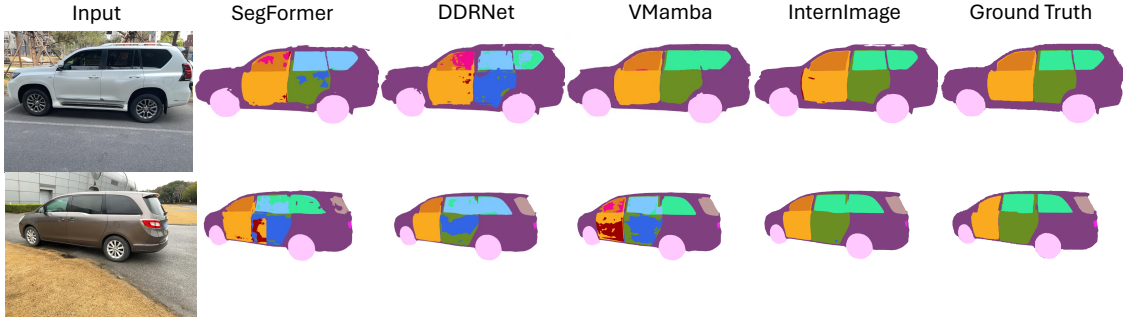


Figure 7. **Qualitative comparisons among recent advanced image segmentation methods.** We select the inputs from the testing set of our images and evaluate the capacity of car component understanding for each method.

Table 2. **Detection improvements by simulated data for corner-case scenes.** We leverage lightweight YOLO serial models and recent state-of-the-art models for evaluation. We report the metric by calculating mAP@0.5 on the CODA dataset [21].

Simulated Data	YOLOv5n	YOLOv5s	YOLOv8n	YOLOv8s	CO-DETR	YOLOv12x
1000	0.285	0.341	0.299	0.371	0.465	0.412
2000	0.304	0.357	0.312	0.366	0.481	0.441
3000	0.345	0.389	0.357	0.403	0.517	0.489
4000	0.357	0.408	0.386	0.413	0.551	0.531
5000	0.361	0.426	0.386	0.435	0.582	0.565

5.3. 2D Tasks

Corner-case 2D Detection. To obtain a reliable detector for corner-case scenes, we simulate corner-case scenes with reconstructed cars and synthesize them within a background. Specifically, we leverage a recent large-scale self-driving dataset, Nuscenes [5] to provide background information. After obtaining a simulated corner-case dataset, we can use this dataset to train and obtain a reliable detector robust for corner-case scenes. As shown in Table 2, we employ YOLOv5 and YOLOv8 serial models, CO-DETR [52], and YOLOv12 [43] as our detectors for evaluation. To evaluate the performance of models in corner-case scenes, we leverage the test part of the CODA dataset [21] as our testing set. In particular, when we increase the training simulated data from 500 to 5,000, the performance of detectors improves by a large margin. This phenomenon demonstrates that our simulated data is effective in improving detection performance to corner-case scenes. We provide the visualizations of simulated corner-case scenes in Figure 6. The detailed simulation process and more visualizations can be seen in the supplementary.

2D Car Parsing. We conduct benchmarks for car parsing maps of our dataset using recent segmentation methods, such

Table 3. **Benchmark results on 2D car parsing of our 3DRealCar dataset.** We use recent advanced image segmentation methods [25, 32, 47, 49] to benchmark our dataset.

Method	SegFormer	DDRNet	VMamba	InternImage
mIOU \uparrow	0.541	0.606	0.610	0.671
mAcc \uparrow	0.652	0.732	0.734	0.786

as DDRNet[32], SegFormer[49], VMamba [25], and InternImage [47]. The quantitative performance for these methods on our dataset is summarized in Table 3. Visual comparisons are provided in Figure 7. Our high-quality dataset enables these methods to achieve promising performance, highlighting its potential for application in self-driving systems. In particular, our car parsing annotations encourage self-driving systems to recognize different components of cars in practical scenarios for safer automatic decisions. We believe that our detailed car parsing annotations could significantly contribute to advancing self-driving tasks.

5.4. 3D Tasks

Neural Field-based Novel View Synthesis. As depicted in Table 4, we show benchmark results of recent state-of-the-art neural field methods, such as Instant-NGP [29], 3DGS [18], GaussianShader [15], 2DGS [13], Pixel-GS [51], and 3DGS-MCMC [19] on our dataset. To the standard lighting condition, we can find that recent methods are capable of achieving PSNR more than 27 dB, which means these methods can reconstruct relatively high-quality 3D cars from our dataset. However, the reflective and dark condition results are lower than the standard. These two parts of our 3DRealCar bring two challenges to recent 3D methods. The first challenge is the reconstruction of specular highlights. Due to the particular property of cars, materials of car surfaces are generally

Table 4. **Benchmark results on 3D reconstruction of our 3DRealCar dataset.** We present the 3D reconstruction performance of recent state-of-the-art methods in three lighting conditions, standard, reflective, and dark, respectively. The best results are highlighted.

Method	Standard			Reflective			Dark		
	PSNR \uparrow	SSIM \uparrow	LPIPS \downarrow	PSNR \uparrow	SSIM \uparrow	LPIPS \downarrow	PSNR \uparrow	SSIM \uparrow	LPIPS \downarrow
Instant-NGP [29]	27.31	0.9315	0.1264	24.37	0.8613	0.1962	23.17	0.9152	0.1642
3DGS [18]	27.47	0.9367	0.1001	24.58	0.8647	0.1852	23.51	0.9181	0.1613
GaussianShader [15]	27.53	0.9311	0.1109	25.41	0.8684	0.1423	23.39	0.9172	0.1631
2DGS [13]	27.34	0.9341	0.1095	23.19	0.8509	0.2041	22.63	0.9148	0.1681
Pixel-GS [51]	27.67	0.9391	0.0994	24.81	0.8659	0.1541	23.54	0.9174	0.1617
3DGS-MCMC [19]	27.63	0.9382	0.0986	24.92	0.8681	0.1621	23.63	0.9198	0.1622

Table 5. **Quantitative comparisons of SOTA 3D Generation method, Dreamcraft3D [40] and its improved version by trained on our dataset.** CD denotes Chamfer Distance.

Method	CLIP-I \uparrow	Hausdorff \downarrow	CD \downarrow
Dreamcraft3D	0.812	1.572	0.587
+our dataset	0.847	1.364	0.371



Figure 8. **Visualizations of diffusion-based novel view synthesis.** we compare the results of the recent state-of-the-art diffusion-based method, Zero123-XL [22] and its improvement by training on our dataset. Our dataset provides car-specific prior for the generative model to generate more photorealistic car images.

glossy, which means it would produce plenty of specular highlights if cars are exposed to the sun or strong light. The second challenge is the reconstruction in a dark environment. The training images captured in the dark environment lose plenty of details for reconstruction. Therefore, how to achieve high-quality reconstruction results from these two extremely lighting conditions is a challenge to recent methods. 3D visualizations can be found on our project page. We hope these results can encourage subsequent research for the 3D reconstruction in low-quality lighting conditions.

Diffusion-based Novel View Synthesis. As illustrated in Figure 8, we show visual comparisons of Zero123-XL [22] and our improved version by training on our dataset. As we can see, given input images, we use Zero123-XL and our improved version to synthesize novel views. We can find that Zero123-XL prefers to generate unrealistic texture and geometry, due to the lack of prior for real objects. In contrast, our improved version of Zero123-XL can generate photorealistic geometry and texture, which demonstrates the effectiveness of our dataset.

Single Image to 3D Generation. Not only do we enhance



Figure 9. **Visualizations of single-image-to-3D generation.** we compare the results of the recent state-of-the-art single-image-to-3D method, Dreamcraft3D [41] and its improved version by training on our dataset.

novel view synthesis for diffusion-based models, but we also demonstrate improvements in 3D generation. As depicted in Figure 9, we visualize 3D generation results of the recent state-of-the-art single-image-to-3D method, Dreamcraft3D [41], along with its improved version by our dataset. This figure shows that Dreamcraft3D sometimes fails to generate complete geometry or realistic texture, due to the scarcity of the real car prior. As shown in Table 5, we also show quantitative comparisons of Dreamcraft3D and its improved version. CLIP-I means the similarity of rendered images with the original input. The quantitative and qualitative results indicate our dataset significantly improves 3D generation performance typically in terms of geometry and texture. These results underscore the effectiveness of our 3DRealCar dataset.

6. Conclusion

In this paper, we propose the first large-scale high-quality 3D real car dataset, named 3DRealCar. The collected dense and high-resolution 360-degree views for each car can be used to reconstruct a high-quality 3D car. Extensive experiments demonstrate the efficacy and challenges of our 3DRealCar in 3D reconstruction. Thanks to the reconstructed high-quality 3D cars from our dataset and car-part level annotations, our dataset can be utilized to support various tasks related to cars. In addition, the benchmarking results can serve as baselines for prospective research. Although 3DRealCar currently only has car exterior views, we intend to provide both exterior and interior views in the future to further promote the reconstruction of more intact 3D cars.

References

- [1] Hervé Abdi and Lynne J Williams. Principal component analysis. *Wiley interdisciplinary reviews: computational statistics*, 2(4):433–459, 2010. 4
- [2] Apple, 2021. 2, 4
- [3] Jonathan T Barron, Ben Mildenhall, Matthew Tancik, Peter Hedman, Ricardo Martin-Brualla, and Pratul P Srinivasan. Mip-nerf: A multiscale representation for anti-aliasing neural radiance fields. In *Proceedings of the IEEE/CVF International Conference on Computer Vision*, pages 5855–5864, 2021. 3
- [4] Jonathan T. Barron, Ben Mildenhall, Dor Verbin, Pratul P. Srinivasan, and Peter Hedman. Mip-NeRF 360: Unbounded Anti-Aliased Neural Radiance Fields. *2022 IEEE/CVF Conference on Computer Vision and Pattern Recognition (CVPR)*, pages 5460–5469, 2022. 3
- [5] Holger Caesar, Varun Bankiti, Alex H Lang, Sourabh Vora, Venice Erin Liang, Qiang Xu, Anush Krishnan, Yu Pan, Giancarlo Baldan, and Oscar Beijbom. nuscenes: A multimodal dataset for autonomous driving. In *Proceedings of the IEEE/CVF conference on computer vision and pattern recognition*, pages 11621–11631, 2020. 6, 7
- [6] Angel X Chang, Thomas Funkhouser, Leonidas Guibas, Pat Hanrahan, Qixing Huang, Zimo Li, Silvio Savarese, Manolis Savva, Shuran Song, Hao Su, et al. Shapenet: An information-rich 3d model repository. *arXiv preprint arXiv:1512.03012*, 2015. 1, 3
- [7] Anpei Chen, Zexiang Xu, Andreas Geiger, Jingyi Yu, and Hao Su. Tensorf: Tensorial radiance fields. In *European Conference on Computer Vision*, pages 333–350. Springer, 2022. 3
- [8] Matt Deitke, Dustin Schwenk, Jordi Salvador, Luca Weihs, Oscar Michel, Eli VanderBilt, Ludwig Schmidt, Kiana Ehsani, Aniruddha Kembhavi, and Ali Farhadi. Objaverse: A universe of annotated 3d objects. In *Proceedings of the IEEE/CVF Conference on Computer Vision and Pattern Recognition*, pages 13142–13153, 2023. 1, 3, 5
- [9] Matt Deitke, Ruoshi Liu, Matthew Wallingford, Huong Ngo, Oscar Michel, Aditya Kusupati, Alan Fan, Christian Laforte, Vikram Voleti, Samir Yitzhak Gadre, et al. Objaverse-xl: A universe of 10m+ 3d objects. *Advances in Neural Information Processing Systems*, 36, 2024. 5
- [10] Xiaobiao Du, Haiyang Sun, Ming Lu, Tianqing Zhu, and Xin Yu. Dreamcar: Leveraging car-specific prior for in-the-wild 3d car reconstruction. *IEEE Robotics and Automation Letters*, 2024. 3
- [11] Xiaobiao Du, Yida Wang, and Xin Yu. Mvgs: Multi-view-regulated gaussian splatting for novel view synthesis. *arXiv preprint arXiv:2410.02103*, 2024. 3
- [12] Carlos J García Orellana, Ramón Gallardo Caballero, Horacio M González Velasco, and Francisco J López Aligué. Neusim: a modular neural networks simulator for beowulf clusters. In *Bio-Inspired Applications of Connectionism: 6th International Work-Conference on Artificial and Natural Neural Networks, IWANN 2001 Granada, Spain, June 13–15, 2001 Proceedings, Part II 6*, pages 72–79. Springer, 2001. 3
- [13] Binbin Huang, Zehao Yu, Anpei Chen, Andreas Geiger, and Shenghua Gao. 2d gaussian splatting for geometrically accurate radiance fields. *arXiv preprint arXiv:2403.17888*, 2024. 3, 5, 6, 7, 8
- [14] Xinyu Huang, Xinjing Cheng, Qichuan Geng, Binbin Cao, Dingfu Zhou, Peng Wang, Yuanqing Lin, and Ruigang Yang. The apolloscape dataset for autonomous driving. In *Proceedings of the IEEE conference on computer vision and pattern recognition workshops*, pages 954–960, 2018. 3
- [15] Yingwenqi Jiang, Jiadong Tu, Yuan Liu, Xifeng Gao, Xiaoxiao Long, Wenping Wang, and Yuexin Ma. Gaussianshader: 3d gaussian splatting with shading functions for reflective surfaces. *arXiv preprint arXiv:2311.17977*, 2023. 6, 7, 8
- [16] Heewoo Jun and Alex Nichol. Shap-E: Generating conditional 3D implicit functions, 2023. 4
- [17] Bernhard Kerbl, Georgios Kopanas, Thomas Leimkühler, and George Drettakis. 3d gaussian splatting for real-time radiance field rendering. *ACM Transactions on Graphics (ToG)*, 42(4): 1–14, 2023. 3
- [18] Bernhard Kerbl, Georgios Kopanas, Thomas Leimkühler, and George Drettakis. 3d gaussian splatting for real-time radiance field rendering. *ACM Transactions on Graphics (ToG)*, 42(4): 1–14, 2023. 4, 5, 6, 7, 8
- [19] Shakiba Kheradmand, Daniel Rebain, Gopal Sharma, Weiwei Sun, Jeff Tseng, Hossam Isack, Abhishek Kar, Andrea Tagliasacchi, and Kwang Moo Yi. 3d gaussian splatting as markov chain monte carlo. *arXiv preprint arXiv:2404.09591*, 2024. 7, 8
- [20] Alexander Kirillov, Eric Mintun, Nikhila Ravi, Hanzi Mao, Chloe Rolland, Laura Gustafson, Tete Xiao, Spencer Whitehead, Alexander C Berg, Wan-Yen Lo, et al. Segment anything. *arXiv preprint arXiv:2304.02643*, 2023. 4, 5
- [21] Kaican Li, Kai Chen, Haoyu Wang, Lanqing Hong, Chaoqiang Ye, Jianhua Han, Yukuai Chen, Wei Zhang, Chunjing Xu, Dit-Yan Yeung, et al. Coda: A real-world road corner case dataset for object detection in autonomous driving. *arXiv preprint arXiv:2203.07724*, 2022. 6, 7
- [22] Ruoshi Liu, Rundi Wu, Basile Van Hoorick, Pavel Tokmakov, Sergey Zakharov, and Carl Vondrick. Zero-1-to-3: Zero-shot one image to 3d object. In *Proceedings of the IEEE/CVF International Conference on Computer Vision*, pages 9298–9309, 2023. 4, 5, 6, 8
- [23] Shilong Liu, Zhaoyang Zeng, Tianhe Ren, Feng Li, Hao Zhang, Jie Yang, Chunyuan Li, Jianwei Yang, Hang Su, Jun Zhu, et al. Grounding dino: Marrying dino with grounded pre-training for open-set object detection. *arXiv preprint arXiv:2303.05499*, 2023. 4
- [24] Yuan Liu, Cheng Lin, Zijiao Zeng, Xiaoxiao Long, Lingjie Liu, Taku Komura, and Wenping Wang. Syncdreamer: Generating multiview-consistent images from a single-view image. *arXiv preprint arXiv:2309.03453*, 2023. 5
- [25] Yue Liu, Yunjie Tian, Yuzhong Zhao, Hongtian Yu, Lingxi Xie, Yaowei Wang, Qixiang Ye, and Yunfan Liu. Vmamba: Visual state space model. *arXiv preprint arXiv:2401.10166*, 2024. 5, 6, 7
- [26] Tao Lu, Mulin Yu, Linning Xu, Yuanbo Xiangli, Limin Wang, Dahua Lin, and Bo Dai. Scaffold-gs: Structured 3d gaussians for view-adaptive rendering. *arXiv preprint arXiv:2312.00109*, 2023. 3

- [27] Gal Metzger, Elad Richardson, Or Patashnik, Raja Giryes, and Daniel Cohen-Or. Latent-nerf for shape-guided generation of 3d shapes and textures. In *Proceedings of the IEEE/CVF Conference on Computer Vision and Pattern Recognition*, pages 12663–12673, 2023. 4
- [28] Ben Mildenhall, Pratul P Srinivasan, Matthew Tancik, Jonathan T Barron, Ravi Ramamoorthi, and Ren Ng. Nerf: Representing Scenes As Neural Radiance Fields for View Synthesis. *Communications of the ACM*, 65(1):99–106, 2021. 3
- [29] Thomas Müller, Alex Evans, Christoph Schied, and Alexander Keller. Instant neural graphics primitives with a multiresolution hash encoding. *arXiv:2201.05989*, 2022. 5, 6, 7, 8
- [30] Thomas Müller, Alex Evans, Christoph Schied, and Alexander Keller. Instant neural graphics primitives with a multiresolution hash encoding. *ACM Transactions on Graphics (ToG)*, 41(4):1–15, 2022. 3
- [31] Alex Nichol, Heewoo Jun, Prafulla Dhariwal, Pamela Mishkin, and Mark Chen. Point-E: A System for Generating 3D Point Clouds from Complex Prompts, 2022. 4
- [32] Huihui Pan, Yuanduo Hong, Weichao Sun, and Yisong Jia. Deep dual-resolution networks for real-time and accurate semantic segmentation of traffic scenes. *IEEE Transactions on Intelligent Transportation Systems*, 24(3):3448–3460, 2022. 5, 6, 7
- [33] Ben Poole, Ajay Jain, Jonathan T Barron, and Ben Mildenhall. Dreamfusion: Text-to-3d using 2d diffusion. *arXiv preprint arXiv:2209.14988*, 2022. 5
- [34] Ben Poole, Ajay Jain, Jonathan T Barron, and Ben Mildenhall. Dreamfusion: Text-to-3d using 2d diffusion. *arXiv preprint arXiv:2209.14988*, 2022. 4
- [35] Christian Reiser, Songyou Peng, Yiyi Liao, and Andreas Geiger. Kilonerf: Speeding up neural radiance fields with thousands of tiny mlps. In *Proceedings of the IEEE/CVF International Conference on Computer Vision*, pages 14335–14345, 2021. 3
- [36] Johannes L. Schonberger and Jan-Michael Frahm. Structure-from-motion revisited. In *2016 IEEE Conference on Computer Vision and Pattern Recognition (CVPR)*, 2016. 4, 5
- [37] Ruoxi Shi, Hansheng Chen, Zhuoyang Zhang, Minghua Liu, Chao Xu, Xinyue Wei, Linghao Chen, Chong Zeng, and Hao Su. Zero123++: a single image to consistent multi-view diffusion base model. *arXiv preprint arXiv:2310.15110*, 2023. 4
- [38] Yichun Shi, Peng Wang, Jianglong Ye, Mai Long, Kejie Li, and Xiao Yang. Mvdream: Multi-view diffusion for 3d generation. *arXiv preprint arXiv:2308.16512*, 2023. 1, 3
- [39] Stability.AI. Stable Zero123: Quality 3d object generation from single images. <https://stability.ai/news/stable-zero123-3d-generation>, 2023. 4, 5, 6
- [40] Jingxiang Sun, Bo Zhang, Ruizhi Shao, Lizhen Wang, Wen Liu, Zhenda Xie, and Yebin Liu. Dreamcraft3d: Hierarchical 3d generation with bootstrapped diffusion prior. *arXiv preprint arXiv:2310.16818*, 2023. 6, 8
- [41] Jingxiang Sun, Cheng Peng, Ruizhi Shao, Yuan-Chen Guo, Xiaochen Zhao, Yangguang Li, Yanpei Cao, Bo Zhang, and Yebin Liu. Dreamcraft3d++: Efficient hierarchical 3d generation with multi-plane reconstruction model. *arXiv preprint arXiv:2410.12928*, 2024. 8
- [42] Jiaxiang Tang, Jiawei Ren, Hang Zhou, Ziwei Liu, and Gang Zeng. DreamGaussian: Generative Gaussian splatting for efficient 3d content creation. *arXiv preprint arXiv:2309.16653*, 2023. 5
- [43] Yunjie Tian, Qixiang Ye, and David Doermann. Yolov12: Attention-centric real-time object detectors. *arXiv preprint arXiv:2502.12524*, 2025. 7
- [44] Ultralytics. YOLOv8: A cutting-edge and state-of-the-art (sota) model that builds upon the success of previous yolo versions. <https://github.com/ultralytics/ultralytics?tab=readme-ov-file>, 2023. 5, 6
- [45] Jingkang Wang, Sivabalan Manivasagam, Yun Chen, Ze Yang, Ioan Andrei Bârsan, Anqi Joyce Yang, Wei-Chiu Ma, and Raquel Urtasun. Cadsim: Robust and scalable in-the-wild 3d reconstruction for controllable sensor simulation. *arXiv preprint arXiv:2311.01447*, 2023. 3
- [46] Peng Wang, Yuan Liu, Zhaoxi Chen, Lingjie Liu, Ziwei Liu, Taku Komura, Christian Theobalt, and Wenping Wang. F2-nerf: Fast neural radiance field training with free camera trajectories. *CVPR*, 2023. 3
- [47] Wenhai Wang, Jifeng Dai, Zhe Chen, Zhenhang Huang, Zhiqi Li, Xizhou Zhu, Xiaowei Hu, Tong Lu, Lewei Lu, Hongsheng Li, et al. Internimage: Exploring large-scale vision foundation models with deformable convolutions. In *Proceedings of the IEEE/CVF conference on computer vision and pattern recognition*, pages 14408–14419, 2023. 5, 6, 7
- [48] Pengchuan Xiao, Zhenlei Shao, Steven Hao, Zishuo Zhang, Xiaolin Chai, Judy Jiao, Zesong Li, Jian Wu, Kai Sun, Kun Jiang, et al. Pandaset: Advanced sensor suite dataset for autonomous driving. In *2021 IEEE International Intelligent Transportation Systems Conference (ITSC)*, pages 3095–3101. IEEE, 2021. 3
- [49] Enze Xie, Wenhai Wang, Zhiding Yu, Anima Anandkumar, Jose M Alvarez, and Ping Luo. Segformer: Simple and efficient design for semantic segmentation with transformers. *Advances in neural information processing systems*, 34:12077–12090, 2021. 5, 6, 7
- [50] Jason Zhang, Gengshan Yang, Shubham Tulsiani, and Deva Ramanan. Ners: Neural reflectance surfaces for sparse-view 3d reconstruction in the wild. *Advances in Neural Information Processing Systems*, 34:29835–29847, 2021. 1, 3
- [51] Zheng Zhang, Wenbo Hu, Yixing Lao, Tong He, and Hengshuang Zhao. Pixel-gs: Density control with pixel-aware gradient for 3d gaussian splatting. In *European Conference on Computer Vision*, pages 326–342. Springer, 2024. 7, 8
- [52] Zhuofan Zong, Guanglu Song, and Yu Liu. Detrs with collaborative hybrid assignments training. In *Proceedings of the IEEE/CVF international conference on computer vision*, pages 6748–6758, 2023. 7